

Polymer Chemistry

Accepted Manuscript



This is an *Accepted Manuscript*, which has been through the Royal Society of Chemistry peer review process and has been accepted for publication.

Accepted Manuscripts are published online shortly after acceptance, before technical editing, formatting and proof reading. Using this free service, authors can make their results available to the community, in citable form, before we publish the edited article. We will replace this *Accepted Manuscript* with the edited and formatted *Advance Article* as soon as it is available.

You can find more information about *Accepted Manuscripts* in the [Information for Authors](#).

Please note that technical editing may introduce minor changes to the text and/or graphics, which may alter content. The journal's standard [Terms & Conditions](#) and the [Ethical guidelines](#) still apply. In no event shall the Royal Society of Chemistry be held responsible for any errors or omissions in this *Accepted Manuscript* or any consequences arising from the use of any information it contains.

COMMUNICATION

Spatial and Temporal Control of Drug Release Through pH and Alternating Magnetic Field Induced Breakage of Schiff Base Bonds

Cite this: DOI: 10.1039/x0xx00000x

Received 31st January 2014,
Accepted XXXAlexander E. Dunn^{a,b}, Douglas J. Dunn^{a,b}, Alexander Macmillan^c, Renee Whan^c,
Tim Stait-Gardner^d, William S. Price^d, May Lim^{a*}, Cyrille Boyer^{b*}

DOI: 10.1039/x0xx00000x

www.rsc.org/

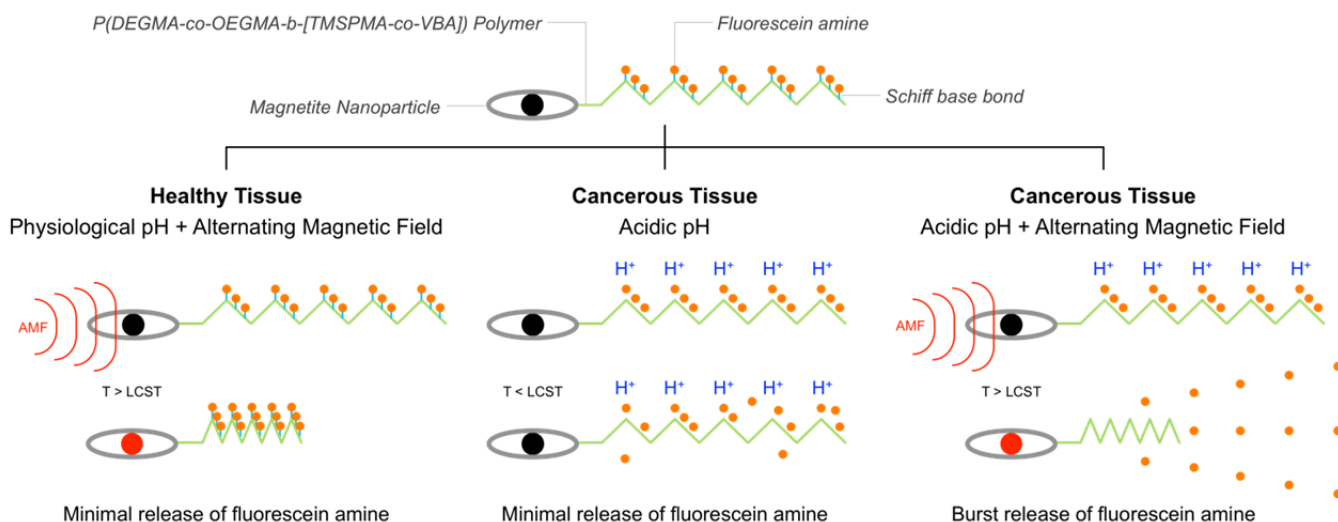
P(DEGMA-co-OEGMA-*b*-[TMSPMA-co-VBA])@Silica@Magnetite polymer-nanoparticle composites have been developed as a platform for controllable drug release. The nanocomposite facilitates controllable release of therapeutic molecules through breakage of pH and heat labile Schiff base bonds that bind the molecules to the polymer. This enables dual-stimuli responsive drug release in response to the acidic microenvironment of cancerous cells and heat generated by the magnetite nanoparticles when subjected to an alternating magnetic field, thereby permitting spatial and temporal control over 'burst' release of the drugs. The nanocomposite has also been shown to be effective at improving magnetic resonance imaging contrast through enhancement of spin-spin relaxivity.

The emergence of nanomedicine is revolutionising the treatment of many diseases, including cancers, cardiovascular diseases and others.¹⁻⁴ Various nanoparticle platforms have been developed for cancer diagnosis and treatment.^{5,6} For example, Langer and co-workers have reported the first clinical trial of targeted polymeric nanoparticles containing the chemotherapeutic docetaxel for the treatment of patients with solid tumours.² Another promising nanoparticle platform involves the use of iron oxide nanoparticles (IONPs) for several applications in medicine, including drug and gene delivery, magnetic resonance imaging (MRI) and hyperthermia therapy.⁷⁻¹² Sophisticated chemistry has also been established to prepare complex polymer-nanoparticle composites, in which a therapeutic agent can be physically loaded or chemically bound to the polymer.¹³⁻¹⁵ The conjugation of therapeutic agents to polymeric layers on IONPs through biologically breakable bonds offers improved control, while the IONP core can be employed as a magnetic resonance imaging contrast agent.⁹

Recently, the application of alternating magnetic fields (AMF) to IONPs loaded with drugs has allowed controllable

release of these drugs through the production of thermal energy by Néel and/or Brownian relaxation.¹⁶⁻²⁰ The use of heat generated to break chemical bonds, thereby allowing the controlled release of therapeutic compounds, presents some advantages as the therapy can be adjusted to the patient's regimen and allows multiple dosages from a single administration.²¹⁻²⁵ It may also help address the importance of timing on therapeutic effect, such as chrono-administration – a new concept that is receiving increasing recognition.²⁶ However, AMF induced release of therapeutic compounds presents several limitations, as it is not specific to diseased tissue. This is an issue in the treatment of diseases such as cancer, where the drug may present some adverse side effects. Fortunately, the difference in physiological properties between diseased and normal tissue, such as the more acidic environment of cancer cells, allows for localised release of drugs when they are sequestered to the drug carrier by a pH responsive bond.²⁷

In this study, we present a new class of polymer-nanoparticle composite based drug carriers that respond simultaneously to both a change in pH and heat generated by AMF to achieve a 'burst' release of fluorescein amine (a model therapeutic molecule) via bond breakage. This unique combination allows temporal and spatial control over the release of the molecules (see Scheme 1). The nanocarrier is constituted by a P(DEGMA-co-OEGMA-*b*-[TMSPMA-co-VBA]) diblock copolymer grafted onto silica coated acicular magnetite nanoparticles (Fe₃O₄). The acicular nanoparticle morphology was chosen as it has been reported to exhibit enhanced cellular uptake²⁸ and bio-circulation²⁹ when compared to its spheroid counterparts. The diblock copolymer confers biocompatibility and colloidal stability, as well as specific functions to covalently attach the molecules through pH and heat labile Schiff base bonds.

P(DEGMA-co-OEGMA-*b*-[TMSPPMA-co-VBA]) grafted magnetite nanoparticle, conjugated with fluorescein amine via Schiff base bond

Scheme 1: Temporal and spatial controlled release of a model therapeutic compound from P(DEGMA-co-OEGMA-*b*-[TMSPPMA-co-VBA]) diblock copolymer grafted onto silica coated acicular magnetite nanoparticles. A) in healthy tissue (pH 7.4), application of an alternating magnetic field causes the particle to heat up above the lower critical solution temperature (LCST) of the polymer, resulting in a contraction of the polymer chains, with a minimal release of the therapeutic compounds due to only partial hydrolysis of Schiff base bonds. B) in cancerous tissue (pH ~ 5.5), an acidic environment causes a slow hydrolysis of Schiff base bonds, again resulting in minimal release of the model therapeutic compound. C) Application of alternating magnetic field (AMF) in acidic environment (such as cancerous tissue) achieves a synergistic effect whereby a rapid hydrolysis of Schiff base bonds is observed due to the increase in temperature and low pH, resulting in a ‘burst’ release of the model therapeutic compound.

The acicular magnetite nanoparticles were synthesised via a three step process. Firstly, acicular hematite (α -Fe₂O₃) nanoparticles were synthesised by forced hydrolysis of iron (III) chloride hexahydrate (0.02 M) in the presence of sodium dihydrogen orthophosphate monohydrate (0.4 mM) and urea (0.01 M) at 100 °C for 18 h.³⁰ A hematite template was employed due to the isotropic nature of magnetite that made it difficult to directly synthesise non-spherical morphologies.³¹ In the second step, a silica layer was introduced using the Stöber method.³² Subsequently, the hematite core was reduced under hydrogen at 500 °C for 5 h to produce the magnetite nanoparticles. The silica layer ensured that the acicular structure was retained after the reduction treatment.

Transmission electron microscopy (TEM) confirmed the successful synthesis of acicular shaped nanoparticles and the presence of a thin coating layer (10 nm) on the nanoparticles after the Stöber process was completed (Figure 1a). X-Ray diffraction crystallography (XRD) of the nanoparticles prior to the hydrogen reduction step revealed characteristic peaks of hematite (Figure 1c). After hydrogen reduction, a new set of peaks that corresponded to magnetite was obtained (Figure 1c). Further, electron microscopy (Figure 1b) and Energy Dispersive X-ray spectroscopy (EDS) (Figure S1) showed sintering of the iron oxide core to form a porous ‘magnetic eye’ structure after the hydrogen reduction step.

The P(DEGMA-co-OEGMA-*b*-[TMSPPMA-co-VBA]) diblock copolymer was synthesised using reversible addition fragmentation chain transfer (RAFT) polymerisation in the presence of 4-cyano-4-(phenylcarbonothioylthio)pentanoic acid as the RAFT agent. First, a P(DEGMA-co-OEGMA) polymer ($M_n=13,500$ g mol⁻¹, PDI=1.19, DEGMA:OEGMA=70:30 in mol%) was synthesised by copolymerisation of poly(ethylene

glycol) methyl ether methacrylate (OEGMA, with MW = 300 g/mol) with di(ethylene glycol) methyl ether methacrylate (DEGMA). This precursor polymer was primarily designed to improve biocompatibility and colloidal stability. Poly(ethylene glycol) methyl ether methacrylate has previously been shown to enhance the stability of nanoparticles by preventing agglomeration through increased steric repulsions, and enhanced biological half-life by assisting in evasion of the reticuloendothelial system.³³ Additionally, copolymerisation of OEGMA with DEGMA conferred temperature responsive properties to the polymer with a lower critical solution

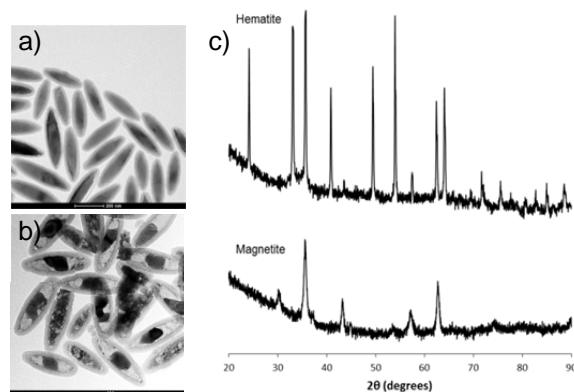


Figure 1: Transmission electron microscopy images of (a) silica coated hematite, (b) silica coated magnetite with sintered ‘eye-like’ structure, and (c) X-ray diffraction spectra of hematite nanoparticles and silica coated magnetite nanoparticles.

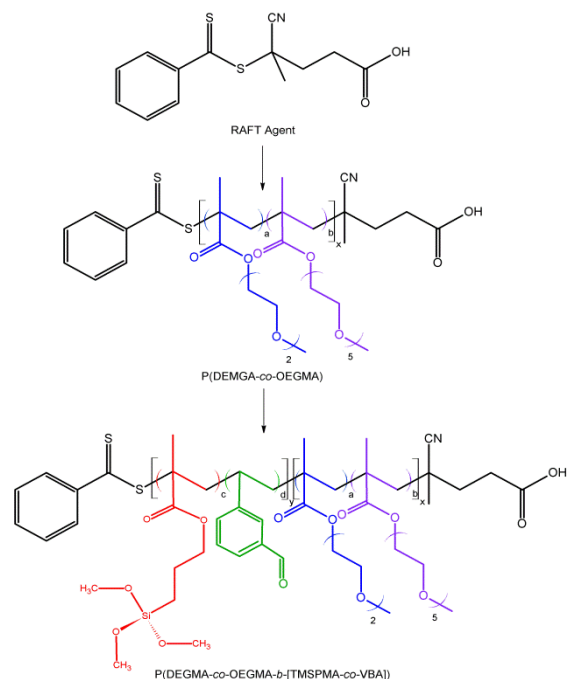


Figure 2: Polymerisation reaction scheme of P(DEGMA-co-OEGMA-*b*-[TMSPMA-co-VBA]) copolymer using RAFT polymerisation.

temperature (LCST) as demonstrated by Lutz and co-workers^{33,34} and others.³⁵ The LCST value of this polymer is slightly lower than values reported in these previous publications. This difference has been attributed to the use of OEGMA with shorter OEG segments (5 units in this work), resulting in a shift to a lower LCST (around 39 °C) (Figure S3). At temperatures above the LCST, the DEGMA-co-OEGMA block will contract allowing molecules trapped within the polymer layer to be released more rapidly. The polymer was subsequently chain extended with 3-(trimethoxysilyl)propyl methacrylate (TMSPMA) and 3-vinylbenzaldehyde (VBA) to yield the final P(DEGMA-co-OEGMA-*b*-[TMSPMA-co-VBA]) diblock copolymer ($M_n=15,000 \text{ g mol}^{-1}$, PDI=1.30, VBA:TMSPMA=80:20 in mol%). Previous works using the polymer containing trimethoxysilyl and benzaldehyde groups have been shown to be non-toxic for a large range of cells.^{9,36,37} The successful chain extension was confirmed by the presence of new signals at 7 and 10 ppm assessed by NMR analysis (Figure S4) and by a shift of the molecular weight distribution as determined by gel permeation chromatography (GPC) (Figure S5). The reaction scheme is shown in Figure 2.

Subsequently, the polymer was grafted onto the acicular magnetite nanoparticles through a reaction between the trimethoxysilane group on the polymer chain and Si-OH group on the nanoparticle surface. The presence of the polymer on the nanoparticle surface was confirmed by X-Ray Photoelectron Spectroscopy (XPS) (Table S1) which showed the presence of new C-O, C=O and O=C-O signals after the grafting and multiple washing steps. Fourier Transform Infrared Spectroscopy (FTIR) further revealed the presence of characteristic carbonyl ester bonds at 1735 cm^{-1} (Figure S6). A polymer grafting density of 0.085 chains per nm^2 was calculated by thermogravimetric analysis (Figure S7), using the surface area assessed by Brunauer-Emmett-Teller (BET)

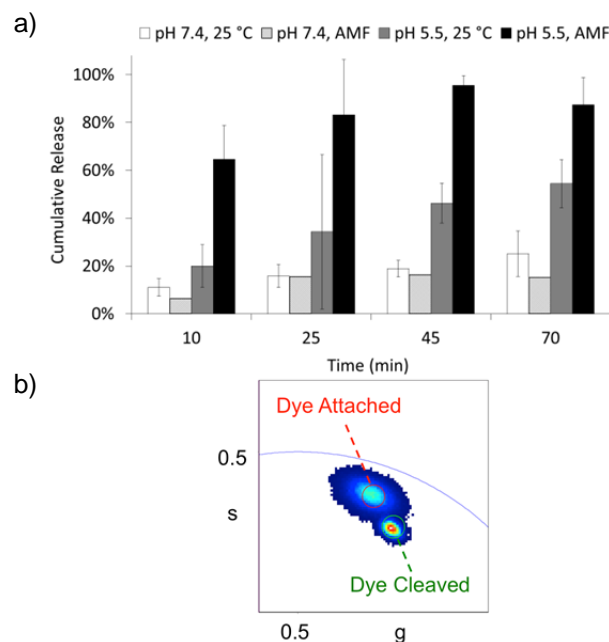


Figure 3: (a) Fluorescein amine release kinetics under physiological (pH 7.4) or acidic (pH 5.5) conditions, with and without the application of an alternating magnetic field. (b) Superposition of two phasor plots from Fluorescence-Lifetime Imaging Microscopy (FLIM) of the nanocarriers with the fluorescein amine dye attached and cleaved. A notable shift in distribution peaks indicates that the dye has been successfully loaded onto the surface of the nanoparticles.

theory. TEM showed that the polymer-grafted nanoparticles are more dispersed than their bare nanoparticle counterpart (Figure S8); dynamic light scattering (DLS) measurements gave a hydrodynamic diameter of $317 \pm 10 \text{ nm}$ in water at pH 7.4, 25 °C.

Conjugation of a model molecule (fluorescein amine) to the polymer-nanoparticle composites was achieved through formation of Schiff base bonds between the primary amine of the dye molecule and the aldehyde on the VBA units in the polymer in the presence of triethylamine as the catalyst, as described in the literature.³⁷ Subsequently, the nanoparticles were purified by at least ten cycles of washing and magnetic separation with 0.1 M NaCl solution to remove any physisorbed fluorescein amine. A reduction in intensity of the aldehyde peak at 10 ppm in the ^1H NMR spectra after reaction with fluorescein amine indicated the successful formation of Schiff base bonds between the polymer and the amine group on the model molecules (Figure S4). Using the poly(ethylene glycol) peak at 4.2 ppm as an internal reference, we were able to quantify a conjugation yield of $84 \pm 2\%$ from the change in ratios of the 10 ppm and 4.2 ppm peaks before and after conjugation.

Studies on the pH and alternating magnetic field induced release of fluorescein amine were carried out by first preparing four samples of the polymer-nanoparticle composite loaded with fluorescein amine (1.75 mg mL^{-1}); two samples were held at physiological pH (pH 7.4), and two at acidic pH (pH 5.5). For each pH, one sample was held at 25 °C, and the other was exposed to the alternating magnetic field (195 kHz, 90 kA/m). Samples that were exposed to acidic pH and alternating magnetic field were found to release the fluorescein amine more rapidly (Figure 3a) than samples exposed to only one

stimulus. A very slow hydrolysis of the Schiff base bonds was observed in an aqueous solution at pH 7.4 and at room temperature. This is because the imine bond is stable at physiological pH and presents slow hydrolysis kinetics. A 'burst' release was observed for samples that were exposed to both stimuli simultaneously; 82% release was achieved within 25 min, as opposed to less than 45% when only a pH stimulus was used. To confirm that the rapid release of the Schiff base was due to the simultaneous effect of the temperature and pH, we measured the release of the fluorescein amine conjugated to polymers via a Schiff Base bond at 25 and 60 °C at pH 5.5. The hydrolysis rate of the Schiff base bond is accelerated by an increase in a temperature in acidic environment (see Figures S9 and S10). Therefore, the rate at which the bond is hydrolysed under acidic conditions can be accelerated by heat induced within the magnetite nanoparticles by the alternating magnetic field. In addition, upon reaching the LCST the polymer contracts and subsequently pushes the fluorescein amine compound out of the polymer layer. Successful release of fluorescein amine (model compound) from the agent was further confirmed by fluorescent lifetime imaging microscopy (Figure 3b). Fluorescein amine conjugated to the nanoparticles displayed a longer lifetime prior to release, however after release a shift to shorter life time was observed, as indicated in the phasor plot (Figure 3).³⁸

Finally, the efficacy of this polymer-nanoparticle composite as an MRI contrast agent was assessed through spin-spin relaxivity measurements. A Bruker Avance 11.7 T wide-bore spectrometer was used to measure the spin-spin relaxivity at various concentrations 0.00-0.10 g L⁻¹ of the nanocomposite (Figure 4). It was found that the relaxivity of the nanocarriers is 86.2 mM⁻¹s⁻¹ at 11.7 T. This value is relatively modest compared to previous values reported in the literature.^{36,39-42} For instance, Kim et al. reported a value of 166 mM⁻¹s⁻¹ at 7 T.⁴²

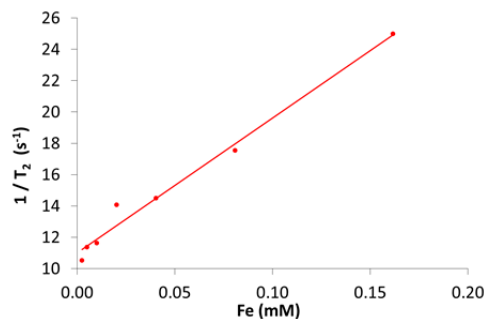


Figure 4: spin-spin relaxivity measurement of polymer-nanoparticle composites in agar gel at different iron concentrations.

Conclusions

In summary, we have demonstrated the use of Schiff base bonds for the conjugation and dual-responsive controllable release of a model for a cancer drug (fluorescein amine) from a polymer-nanoparticle composite. We have shown that the rate at which this pH labile bond is hydrolysed is controlled through temperature and pH, thus providing a mechanism that allows 'burst' release of drug molecules through alternating magnetic

field induced heating. The model drug is rapidly released in an acidic microenvironment under an alternating magnetic field. In healthy tissues (pH ~7.4), the amount and/or rate of drug released is low and/or slow such that the drug cannot accumulate and cause damage to the cell, thus minimising the adverse effects of some cancer treatments. Finally, we demonstrated that this agent was effective as a theranostic agent through enhancement of MRI T_2 relaxivity. In future work, we will investigate the conjugation of doxorubicin and its release using this concept.

Notes and references

^a ARC Centre of Excellence for Functional Nanomaterials, School of Chemical Engineering, The University of New South Wales, Sydney NSW 2052, Australia

^b Australian Centre for NanoMedicine and Centre for Advanced Macromolecular Design, School of Chemical Engineering, The University of New South Wales, Sydney NSW 2052, Australia

^c Biomedical Imaging Facility, Mark Wainwright Analytical Centre, The University of New South Wales, Sydney NSW 2052, Australia

^d Nanoscale Organisation and Dynamics Group, School of Science and Health, University of Western Sydney, Penrith NSW 2751, Australia

We thank the UNSW Mark Wainwright Analytical Centre for provision of characterisation facilities, in particular Dr Rhiannon Kuchel from the Electron Microscopy Unit for her assistance with Energy Dispersive X-ray Spectroscopy analysis. We would also like to thank Mr Jiunn Lee of the University of New South Wales for executing the VSM measurements. The authors also acknowledge the facilities and the scientific and technical assistance of the National Imaging Facility, University of Western Sydney Node.

† Electronic Supplementary Information (ESI) available: [details of any supplementary information available should be included here]. See DOI: 10.1039/c000000x/

(1) Duncan, R.; Gaspar, R. *Molecular Pharmaceutics* **2011**, *8*, 2101-2141.

(2) Hrkach, J.; Von Hoff, D.; Ali, M. M.; Andrianova, E.; Auer, J.; Campbell, T.; De Witt, D.; Figa, M.; Figueiredo, M.; Horhota, A.; Low, S.; McDonnell, K.; Peeke, E.; Retnarajan, B.; Sabnis, A.; Schnipper, E.; Song, J. J.; Song, Y. H.; Summa, J.; Tompsett, D.; Troiano, G.; Van Geen Hoven, T.; Wright, J.; LoRusso, P.; Kantoff, P. W.; Bander, N. H.; Sweeney, C.; Farokhzad, O. C.; Langer, R.; Zale, S. *Science Translational Medicine* **2012**, *4*, 128-139.

(3) Eliasof, S.; Lazarus, D.; Peters, C. G.; Case, R. I.; Cole, R. O.; Hwang, J.; Schluep, T.; Chao, J.; Lin, J.; Yen, Y.; Han, H.; Wiley, D. T.; Zuckerman, J. E.; Davis, M. E. *Proceedings of the National Academy of Sciences* **2013**, *110*, 15127-15132.

(4) Prabhakar, U.; Maeda, H.; Jain, R. K.; Sevic-Muraca, E. M.; Zamboni, W.; Farokhzad, O. C.; Barry, S. T.; Gabizon, A.; Grodzinski, P.; Blakey, D. C. *Cancer Research* **2013**, *73*, 2412-2417.

(5) Doane, T. L.; Burda, C. *Chemical Society Reviews* **2012**, *41*, 2885-2911.

(6) Parveen, S.; Misra, R.; Sahoo, S. K. *Nanomedicine: Nanotechnology, Biology and Medicine* **2012**, *8*, 147-166.

- (7) Fang, C.; Kievit, F. M.; Veiseh, O.; Stephen, Z. R.; Wang, T.; Lee, D.; Ellenbogen, R. G.; Zhang, M. *Journal of Controlled Release* **2012**, *162*, 233-241.
- (8) Boyer, C.; Bulmus, V.; Priyanto, P.; Teoh, W. Y.; Amal, R.; Davis, T. P. *Journal of Materials Chemistry* **2009**, *19*, 111-123.
- (9) Boyer, C.; Whittaker, M. R.; Bulmus, V.; Liu, J.; Davis, T. P. *NPG Asia Mater* **2010**, *2*, 23-30.
- (10) Laurent, S.; Bridot, J.-L.; Elst, L. V.; Muller, R. N. *Future Medicinal Chemistry* **2010**, *2*, 427-449.
- (11) Laurent, S.; Dutz, S.; Häfeli, U. O.; Mahmoudi, M. *Advances in Colloid and Interface Science* **2011**, *166*, 8-23.
- (12) N'Guyen, T. T. T.; Duong, H. T. T.; Basuki, J.; Montebault, V.; Pascual, S.; Guibert, C.; Fresnais, J.; Boyer, C.; Whittaker, M. R.; Davis, T. P.; Fontaine, L. *Angewandte Chemie International Edition* **2013**, n/a-n/a.
- (13) El-Dakdouki, M. H.; Pure, E.; Huang, X. *Nanoscale* **2013**, *5*, 3895-3903.
- (14) Yu, M. K.; Jeong, Y. Y.; Park, J.; Park, S.; Kim, J. W.; Min, J. J.; Kim, K.; Jon, S. *Angewandte Chemie International Edition* **2008**, *47*, 5362-5365.
- (15) Boyer, C.; Priyanto, P.; Davis, T. P.; Pissuwan, D.; Bulmus, V.; Kavallaris, M.; Teoh, W. Y.; Amal, R.; Carroll, M.; Woodward, R.; St Pierre, T. *Journal of Materials Chemistry* **2010**, *20*, 255-265.
- (16) Mahmoudi, M.; Sant, S.; Wang, B.; Laurent, S.; Sen, T. *Advanced Drug Delivery Reviews* **2011**, *63*, 24-46.
- (17) Laurent, S.; Forge, D.; Port, M.; Roch, A.; Robic, C.; Vander Elst, L.; Muller, R. N. *Chemical Reviews* **2008**, *108*, 2064-2110.
- (18) Zhao, X.; Kim, J.; Cezar, C. A.; Huebsch, N.; Lee, K.; Bouhadir, K.; Mooney, D. J. *Proceedings of the National Academy of Sciences* **2010**.
- (19) Kong, S. D.; Zhang, W.; Lee, J. H.; Brammer, K.; Lal, R.; Karin, M.; Jin, S. *Nano Letters* **2010**, *10*, 5088-5092.
- (20) Dunn, A. E.; Dunn, D. J.; Lim, M.; Boyer, C.; Thanh, N. T. K. In *Nanoscience: Volume 2*; The Royal Society of Chemistry: 2014; Vol. 2, p 225-254.
- (21) Qiao, R.-R.; Zeng, J.-F.; Jia, Q.-J.; Du, J.; Shen, L.; Gao, M.-Y. *Wuli Huaxue Xuebao* **2012**, *28*, 993-1011.
- (22) Tong, R.; Hemmati, H. D.; Langer, R.; Kohane, D. S. *Journal of the American Chemical Society* **2012**, *134*, 8848-8855.
- (23) Ramishetti, S.; Huang, L. *Therapeutic Delivery* **2012**, *3*, 1429-1445.
- (24) Shao, Y.; Huang, W.; Shi, C.; Atkinson, S. T.; Luo, J. *Therapeutic Delivery* **2012**, *3*, 1409-1427.
- (25) Steinbach, O. C. *Therapeutic Delivery* **2012**, *3*, 1373-1377.
- (26) Jain, R. K. *Nat Med* **2001**, *7*, 987-989.
- (27) Tannock, I. F.; Rotin, D. *Cancer Research* **1989**, *49*, 4373-4384.
- (28) Doshi, N.; Mitragotri, S. *Journal of The Royal Society Interface* **2010**, *7*, S403-S410.
- (29) Yang, K.; Ma, Y. *Nature Nanotechnology* **2010**, *5*, 579-583.
- (30) Ocaña, M.; Morales, M. P.; Serna, C. J. *Journal of Colloid and Interface Science* **1999**, *212*, 317-323.
- (31) Chen, S.; Feng, J.; Guo, X.; Hong, J.; Ding, W. *Materials Letters* **2005**, *59*, 985-988.
- (32) Stöber, W.; Fink, A.; Bohn, E. *Journal of Colloid and Interface Science* **1968**, *26*, 62-69.
- (33) Lutz, J.-F.; Hoth, A. *Macromolecules* **2005**, *39*, 893-896.
- (34) Lutz, J.-F.; Akdemir, Ö.; Hoth, A. *Journal of the American Chemical Society* **2006**, *128*, 13046-13047.
- (35) Soeriyadi, A. H.; Li, G.-Z.; Slavin, S.; Jones, M. W.; Amos, C. M.; Becer, C. R.; Whittaker, M. R.; Haddleton, D. M.; Boyer, C.; Davis, T. P. *Polymer Chemistry* **2011**, *2*, 815-822.
- (36) Basuki, J. S.; Duong, H. T. T.; Macmillan, A.; Erlich, R. B.; Esser, L.; Akerfeldt, M. C.; Whan, R. M.; Kavallaris, M.; Boyer, C.; Davis, T. P. *ACS Nano* **2013**, *7*, 10175-10189.
- (37) Liu, J.; Duong, H.; Whittaker, M. R.; Davis, T. P.; Boyer, C. *Macromolecular Rapid Communications* **2012**, *33*, 760-766.
- (38) Digman, M. A.; Caiolfa, V. R.; Zamai, M.; Gratton, E. *Biophysical Journal* **2008**, *94*, L14-L16.
- (39) Basuki, J. S.; Esser, L.; Zetterlund, P. B.; Whittaker, M. R.; Boyer, C.; Davis, T. P. *Macromolecules* **2013**, *46*, 6038-6047.
- (40) Basuki, J. S.; Jacquemin, A.; Esser, L.; Li, Y.; Boyer, C.; Davis, T. P. *Polymer Chemistry* **2014**, DOI: 10.1039/C1033PY01778H.
- (41) Basuki, J. S.; Esser, L.; Duong, H. T. T.; Zhang, Q.; Wilson, P.; Whittaker, M. R.; Haddleton, D. M.; Boyer, C.; Davis, T. P. *Chemical Science* **2014**, *5*, 715-726.
- (42) Kim, H.; Dae, H.-M.; Park, C.; Kim, E. O.; Kim, D.; Kim, I.-H.; Kim, Y.-H.; Choi, Y. *Journal of Materials Chemistry* **2011**, *21*, 7742-7747.

Text for Table of Contents

A novel theranostic controlled drug delivery platform that binds the drug to the nanocarrier by utilising Schiff base bonds to achieve high spatial and temporal control over drug release.

